diation viewed opposite edges of the exhaust from a site about 70 ft from the engine, and the resulting sonagrams showed that both radiometers observed the same frequency (1750 Hz). Phase analysis was accomplished via a dual-beam oscilloscope, and Fig. 7 shows that the two radiometer signals were 180° out of phase. This indicates a tangential rather than radial mode of instability.

References

[1] "Evaluation of Combustion Instability Detection Techniques," AFRPL-TR-65-44, May 1965, Aerojet-General Inc., Sacramento, Calif.

[2] Combs, L. P. et al., "Improvement of Bombs and Pulse Guns as Combustion Stability Rating Devices," AFRPL-TR-68-18, March 1968, Rocketdyne, A Div. of North American Rockwell Corp., Canoga Park, Calif.

[3] O'Neill, R. J., Dodson, H. C., and Forman, L. S., "Test Report—One-Tenth Segment XRL Model Rocket Tests," CDM 8121-5002, Jan. 1968, Rocketdyne, A Div. of North American Rockwell Corp., Canoga Park, Calif.

[4] "Advanced Engine Aerospike, Experimental Program," Interim Report R-7475, Vol. II, June 1968, Rocketdyne, A Div. of North American Rockwell Corp., Canoga Park, Calif.

Comparison of Predicted and Measured Low-Density Plume Impingement Effects

L. M. Shaw* and R. S. Hickman†
McDonnell Douglas Corporation, Huntington Beach, Calif.

Nomenclature

C_H	=	Stanton number
C_m	=	molecular thermal speed
$\mathfrak{M}$	=	molecular mass
$\dot{N}$	=	molecular collision rate
P_w	=	pressure
$\dot{q}$	=	heat flux
R	=	gas constant
Re	=	Reynolds number
S	=	molecular speed ratio
T	=	temperature
v	=	directed velocity
x	=	distance along streamline
γ	=	ratio of specific heats
δ	=	geometric scale factor
η	=	number density
θ_i	=	impingement angle
λ	=	mean free path
ρ	=	density
σ^2	=	molecular collision cross section

Subscripts

ex, f	=	exit and flight, respectively
i,j,m	=	incident, jet, and modeled, respectively
o,w,∞	=	total, wall, and ambient, respectively

Introduction

THE behavior of freely expanding plumes has received considerable attention. Aerodynamicists have investigated the behavior of sonic orifices as sources for molecular beams or as primary sources of test gas for conventional flow measurements in high Mach number/low-density flow experiments.[1–3] However, the details of flowfields impinging on surfaces placed in a near-free molecular flow are difficult to determine for well defined flowfields and virtually impossible for rarefied freely expanding jets. The details of such noncontinuum expansion are the subject of current research.[4–6] The work presented was done to define loads and heat transfer to the Saturn V/S-IVB J-2 engine during orbital operation of an oxygen-hydrogen burner engine. The most critical parameter was the heating rate to the J-2 engine, which needed to be defined to insure engine restart capability.

To achieve flowfield simulation, M_{ex}, T_0, Re_{ex} should be matched, the nozzle must be duplicated, and geometry should be duplicated. (The latter two relate to the effect of the nozzle boundary layer.) By simulating flowfield M's and local unit Re's, flowfield Knudsen numbers are duplicated. Duplication of flow chemistry is impossible unless the actual combustion gases are used. Since this normally involves the release of H_2, which cannot be readily pumped cryogenically, test gases must be used that can be condensed with 20° to 30°K helium cryogenic surfaces. As a result, the γ and $\mathfrak{M}$ of the test gas normally will not be the same as the flight gas. Finally, T_0/T_w should be held fixed to duplicate the behavior of the hypersonic flow near the surface.

Simultaneous simulation of M, T_0, and Re can be achieved either by a full-scale test or by a reduced scale with increased density. For a scaled condition,

$$\rho_f/\rho_m = \delta\ \mathfrak{M}_f\sigma^2{}_m/\mathfrak{M}_m\sigma^2{}_f \qquad (1)$$

where δ is the geometric scale factor. To assure a similar limiting velocity, T_0 must be duplicated.

Plume Limitations

Several facility-generated problems can arise in low-density, noncontinuum expansions.[4–7] Of special concern is the permeation of ambient molecules into the stimulated flowfield.

Several regimes can be recognized in a rarefied plume. Near the origin for a continuum source (i.e., $\lambda^* \ll r^*$, where the flow is sonic) the flow will be completely controlled by collisions between molecules in the jet. Some dissipation will be present due to viscous stresses in the jet, but they will not significantly alter the velocity, and the increase in gas temperature can be neglected, since the increase in random kinetic energy will be much less than the average directed kinetic energy. The second regime is that portion of the flow in which collisions with static ambient gas occur with the same frequency as collisions between jet molecules. Here the external gas will begin to scatter the plume molecules causing a degradation of the plume flow properties. Finally, after the jet has expanded to an extremely low density, collisions with the ambient gas will be more important than between jet molecules. This essentially two-fluid model of the gaseous expansion assumes that the ambient

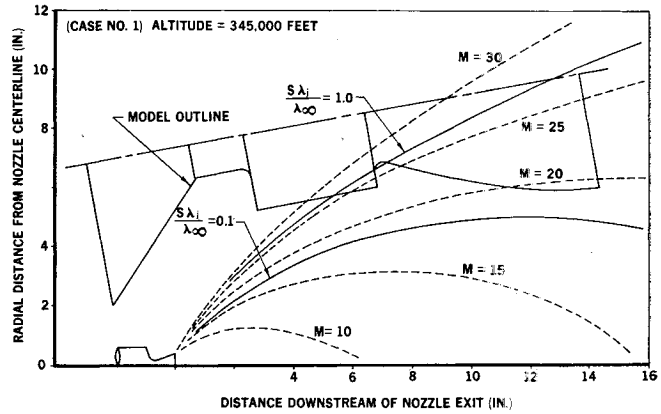

Fig. 1 Nitrogen plume flowfield from method of characteristics solution.

Received August 11, 1969.

* Engineer/Scientist Specialist, MOL Aero/Thermodynamics Section.

† Consultant; also, Associate Professor, Mechanical Engineering Department, University of California at Santa Barbara. Member AIAA.

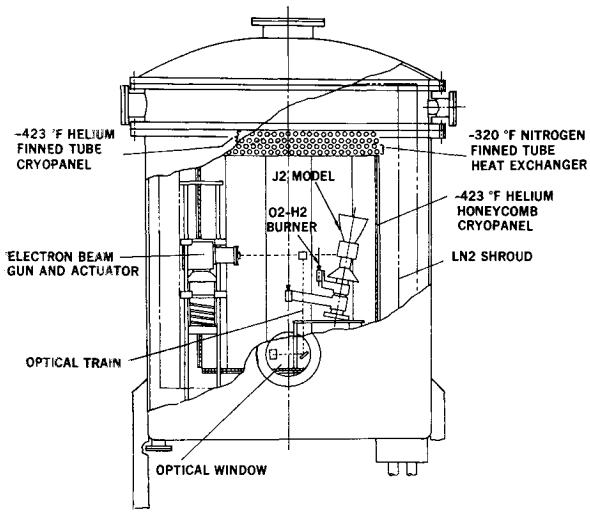

Fig. 2 Space simulation chamber and test equipment.

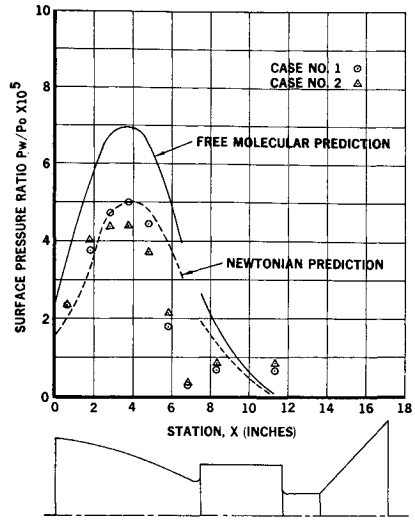

Fig. 3 Surface pressure divided by nozzle chamber pressure vs station along plane of symmetry for test conditions. Case 1 has full simulation, case 2 failed to simulate Knudsen numbers.

gas permeates the entire flowfield to decelerate the jet molecules; it does not accurately describe the flow near the orifice or nozzle because in this region continuum flow dominates and little or no deceleration exists.

With the assumption of a two-fluid model it is possible to develop an approach to define the amount of background molecule permeation. If we define $\dot{N}_\infty$ ($\simeq v/\lambda_\infty$) to be the rate of collisions between a jet molecule and the assumed stationary ambient molecules, and $\dot{N}_j$ ($\simeq C_m/\lambda_j$) as the rate of collisions between a jet molecule and other jet molecules, then we can estimate the jet number density decay as

$$\left.\frac{d\eta_j}{dt}\right|_{\text{jet}} = \frac{d\eta_j}{dx}\,v = -P_m\eta_j\eta_\infty\sigma^2 v = -\frac{S\lambda_j}{\lambda_\infty}\,\eta_j\eta_\infty\sigma^2 v \qquad (2)$$

where P_m is the probability that a jet molecule will be cast from the jet due to a collision with an ambient molecule, and we assume that $P_m = \dot{N}_\infty/(\dot{N}_j + \dot{N}_\infty)$. We are thus modeling the collision process to allow some scattered jet molecules to be restored to the jet flow. Also we assume that $\dot{N}_j \gg \dot{N}_\infty$. Replacing $\sigma^2\eta_\infty = 1/\lambda_\infty$ and integrating gives

$$\frac{\eta_j'}{\eta_j} = \frac{\rho_j'}{\rho_j} = e^{-\int_0^x (S\lambda_j/\lambda_\infty)(dx/\lambda_\infty)} \qquad (3)$$

where the primed terms represent the values after being depleted by ambient permeation.

For a test to simulate flight conditions, the exponential decay distance $S\lambda_j/\lambda_\infty$ must be small for both flows. We have taken $S\lambda_j/\lambda_\infty = 1.0$ as a limiting case for permeation. This limit is illustrated in Fig. 1, which represents a test condition for the simulated O_2-H_2 burner (nitrogen) plume impinging upon model J-2 engine configuration. The effects were expected to be insignificant, since it is found that $S\lambda_j/\lambda_\infty < 1$ near the impingement surface.

Description of Experiment and Instrumentation

A test simulating the impingement of the O_2-H_2 burner onto the Saturn V/S-IVB J-2 engine was conducted in the McDonnell Douglas Corporation 5- × 6-ft space simulation chamber (Fig. 2).[8] Use of a 2-kw helium cryopumping refrigeration system allowed continuous flow from the scaled gas source at chamber pressures corresponding to a 300,000 to 600,000 ft altitude, through the use of two 20-in., oil-diffusion pumps backed by a rotary mechanical pump. The vacuum capability was enhanced by a complete liquid nitrogen shroud and helium cryopanels that operate at 20° to 24°K.

Two 0.1-scale J-2 engine models were used, model 1 for measuring surface pressure and heat flux and model 2 for use with an electron beam probe for measuring flow densities. Each model was cast from aluminum with cooling coils imbedded in the casting to provide cooling of the model surface to 140° and 460°R using liquid nitrogen and Freon, respectively. On model 1, ten pressure orifices (using an orificed cavity configuration) distributed along the instrumentation line, were read through the use of a scanner valve and a 1-mm, MKS baratron pressure instrument. Heat flux measurements were obtained from five Hy-Cal calorimeters distributed along the instrumentation line. Model 2 was instrumented with Faraday cups to enable the reading of beam current and provide focusing of the beam onto the model. This also reduced secondary electron back-scattering from the surface. The gas densities in the plume and impingement region were obtained by measuring electron-beam-induced fluorescence in nitrogen. The fluorescence emitted by the plume molecules excited by a 10 kev electron beam was observed by a photomultiplier tube. For a constant beam current the emitted radiation at a point on the beam is directly proportional to the local number density of the molecules in their ground state.[8,9]

Results and Discussion

In flow regimes under consideration (i.e., free molecular, transition, and slip flow), heat flux to a surface can be expressed by[10]

$$\dot{q} = C_H(\rho_i v^3/2)\sin\theta_i\{1 - [(\gamma+1)/2\gamma]T_w/T_0\} \qquad (4)$$

Total accommodation between molecular-surface interaction

Table 1 Operating parameters at $M_{ex} = 4.6$

	Re_{ex}	λ_{ex}, in.	γ_{ex}	P_0, psia	T_0, °R	T_w, °R	Gas
Flight	2.52×10^4	3.42×10^{-3}	1.46	4.00	1500	460	H_2O, H_2
Test 1	2.67×10^4	3.42×10^{-4}	1.40	27.32	1512	464	N_2
Test 2	1.23×10^4	6.64×10^{-4}	1.40	12.20	1311	460	N_2

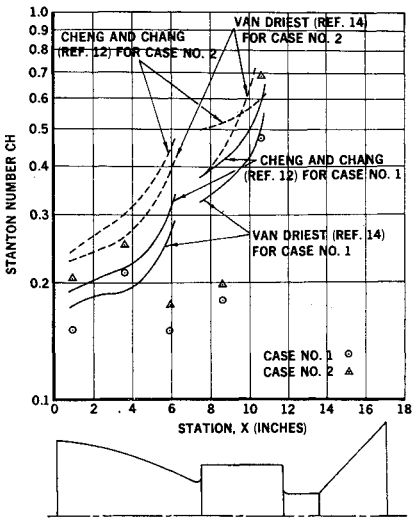

Fig. 4 Stanton number vs station along plane of symmetry for test conditions. Case 1 has full simulation, case 2 failed to simulate Knudsen numbers.

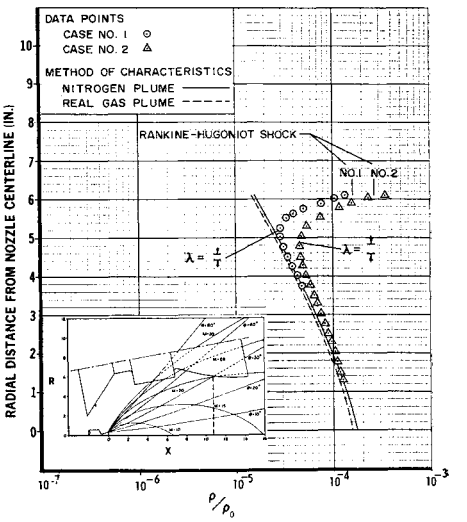

Fig. 5 Density ratio traverse through the plume flowfield.

and hyperthermal flow were assumed; therefore, the reflected temperature is just T_w. The pressure on a surface placed in a hypersonic free molecular flow is, for complete accommodation and assuming a hyperthermal limit,

$$P_w = \rho_i v^2 \sin^2\theta_i + (\rho_i/2)v \sin\theta_i (2\pi R T_w)^{1/2} \qquad (5)$$

Table 1 presents the conditions for two tests designed to: 1) simulate closely the flight conditions (to permit comparisons of experimental results and predictions, and to obtain the desired flight Stanton numbers and pressure correlations), and 2) scale corresponding tests (whose conditions differ) to illustrate the use of Cheng's and Chang's results[11] for heating rate.

Figure 3 compares test data for P_w/P_0 with the plume flowfield values computed by the method of characteristics.[12] The data fall below the free-molecular solution, as should be expected, and approach the Newtonian solution. The data between stations 5 and 8 do not follow this trend and fall well below the Newtonian solution; however, this location on the body surface exists in a separated flow region. No pressure rise due to flow reattachment is apparent in the data near this region, which would indicate that the flow interaction with the surface exists in a noncontinuum regime. It is evident from the data that both plumes exist in a similar flow regime and that neither shows a significant effect of background gas permeation (except, possibly, near stations 10 to 12); this is also implied in Fig. 1.

Figure 4 presents Stanton number (C_H) data over the J-2 engine model for the two test conditions. A corresponding continuum C_H distribution obtained using the method of Van Driest[13] is presented for each case along with predictions using the method discussed by Cheng and Chang.[11] The data agree well with results using both methods, except near the separated flow region, indicating that the flow-body interaction is near a continuum regime. For the test cases, C_H ranged from 0.14 to 0.4 for the J-2 engine bell region, which also agrees with Haslett and Krewski[14] for a low transition regime. Although the Van Driest solution shows slightly better correlation with the data, Cheng and Chang's analysis should be more generally valid for a full range of regimes.

Figure 5 presents the density ratio profile in the plume flowfield along the location indicated by the vertical dashed line (Station 10.8) in the insert. The test data were obtained with electron beam fluorescence techniques and gave results within 10% of those predicted by the method of characteristics. The data were normalized to the predicted undisturbed density to demonstrate the density departure from the undisturbed flow near the surface. The density ratio gradient far from the body agrees with the nitrogen and real-gas characteristic solutions and approaches the Rankine-Hugoniot shock conditions near the surface. The data appear to fit a slip- to continuum-flow picture. The upstream λ is ~0.2 of the adjustment distance for density. The relatively close agreement of the pressure and heat flux data with continuum solutions is, therefore, borne out by the local density data. If the Knudsen number is taken as λ_j/r_b (r_b = local body radius), the values corresponding to the test conditions range from 0.07 to 0.3, which should put the data in the slip- to low-transition regime.

With the v_i's, λ's, T_w's and relative geometry the same as the flight values, it should be expected that the interaction phenomena between the flowfield and body surface would be closely duplicated. Since full-scale testing was impractical, we must rely upon the scaled test to obtain the correct Stanton numbers and pressure correlation. With the absence of background molecule permeation and the ability to predict local freestream plume density, one expects that the calculations using these C_H's and pressure correlations for the flight case will be close to the correct value.

References

[1] French, J. B., "Continuum-Source Molecular Beams," *AIAA Journal*, Vol. 3, No. 6, June 1965, pp. 993–1000.

[2] Ashkenas, H. and Sherman, F. S., "The Structural and Utilization of Supersonic Free Jets in Low Density Wind Tunnels," *Rarefied Gas Dynamics Fourth Symposium*, Vol. II, Academic Press, New York, 1964.

[3] Marrone, P. V., "Rotational Temperature and Density Measurements in Underexpanded Jets and Shock Waves Using an Electron Beam Probe," UTIAS Rept. 113, Jan. 1966, Univ. of Toronto.

[4] Edwards, R. H. and Rogers, A. W., "Steady Nonisentropic Jet Expansion into a Vacuum," AIAA Paper 66–490, Los Angeles, Calif., June 1966.

[5] Edwards, R. H. and Cheng, H. K., "Steady Expansion of a Gas into a Vacuum," *AIAA Journal*, Vol. 4, No. 3, March 1966, pp. 558–561.

[6] Hamel, B. B. and Willis, D. R., "Kinetic Theory of Source Flow Expansion with Application of the Free Jet," *The Physics of Fluids*, Vol. 9, No. 5, May 1966.

[7] Sherman, F. S., "Hydrodynamical Theory of Diffusive Separation of Mixtures in a Free Jet," *The Physics of Fluids*, Vol. 8, No. 5, May 1965.

[8] Nelson, L. A. and Chuan, R. L., "Facility for Simulation of Rocket Plumes in a Space Environment," presented to the IES/AIAA/ASTM Third Space Simulation Conference, Sept. 1968.

[9] Gadamer, E. O., Muntz, E. P., and Patterson, G. N., "Application of an Electron Gun for the Measurement of Density

and Temperature in Rarefied Gas Flows," UTIAS Rept. 73, April 1961, Univ. of Toronto.

[10] Patterson, G. N., "A State of the Art Survey of Some Aspects of the Mechanics of Rarefied Gases and Plasmas," ARL Rept. 64-60, April 1964.

[11] Cheng, H. K. and Chang, A. L., "Hypersonic Shock Layer at Low Reynolds Number—The Yawed Cylinder," ARL 62-453, Oct. 1962.

[12] Vick, A. R. et al., "Comparisons of Experimental Free-Jet Boundaries with Theoretical Results Obtained with the Method of Characteristics," TN D-2327, June 1964, NASA.

[13] Van Driest, E. R., "The Problem of Aerodynamic Heating," *Aeronautical Engineering Review*, Oct. 1956.

[14] Haslett, R. A. and Krewski, T. M., "Plume Heating Due to a Rocket-Engine Exhaust in a High Vacuum," presented at the Aviation and Space Conference, American Society of Mechanical Engineers, Los Angeles, Calif., March 14-18, 1965.

A Simplified Method for Predicting Satellite Passes

KATHLEEN S. BUDLONG*
Bedford Institute, Dartmouth, N.S., Canada

Introduction

IN spite of the many applications of rise and set (alert) times, elevation and azimuth of a satellite in a polar orbit, the author has found very little reference to detailed derivations of these equations. The present Note uses a much simplified approach to derive these equations for the very special case of plane circular polar orbit about a spherical earth. This is the case of the satellites of the Navy Navigation Satellite System (NNSS). A discussion of the errors introduced by these assumptions is presented at the end of the paper.

Derivation of the Basic Equation

The rise time calculations are based on solving the orbit equations for the case of an elevation angle α with respect to the station equal to zero and $d\alpha/dt$ greater than zero.

The elevation must be expressed in terms of known parameters. An NNSS satellite defines its own orbit by describing the plane of the orbit with respect to an XYZ system of coordinates.

In this system the X and Y axes define the plane of the equator, with the X axis pointing toward the vernal equinox. The Z axis is directed north along the earth's axis of rotation

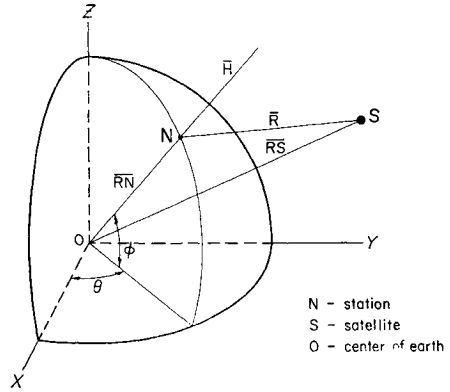

Fig. 1 Position of station N with respect to the XYZ coordinates.

Received June 19, 1969. The author wishes to thank C. D. Maunsell, D. I. Ross, and S. P. Srivastava of the Bedford Institute for valuable suggestions in the preparation of this Note.

* Computers System Analyst.

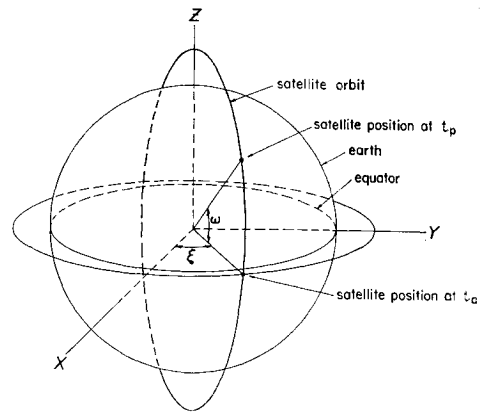

Fig. 2 The satellite orbit referred to the XYZ coordinates.

(Fig. 1). This coordinate system does not rotate with the earth.

The station position can also be referenced to the XYZ system by θ, the station sidereal time, and ϕ, the station latitude. The basic equation will therefore be written, in terms of the XYZ system

$$B = R\sin\alpha = \mathbf{R}\cdot\mathbf{H} \tag{1}$$

where α = elevation angle, measured from the station horizon; $\mathbf{R}$ = slant range vector from the station to the satellite; $R = |\mathbf{R}|$; $\mathbf{H}$ = unit vector at the station pointing toward the station zenith.

The vector $\mathbf{H}$ can be seen from Fig. 1 to have components

$$H_x = \cos\phi\cos\theta,\quad H_y = \cos\phi\sin\theta,\quad H_z = \sin\phi \tag{2}$$

The slant range vector $\mathbf{R}$ can be expressed in terms of the station vector $\mathbf{RN}$ (center of earth to station) and the satellite vector $\mathbf{RS}$ (center of earth to satellite);

$$\mathbf{R} = \mathbf{RS} - \mathbf{RN} \tag{3}$$

$\mathbf{RN}$ has the direction of $\mathbf{H}$ and magnitude R_e, the radius of the earth, and is thus related to the XYZ system without further change;

$$\mathbf{RN} = R_e\mathbf{H} \tag{4}$$

To express $\mathbf{RS}$ we should consider the orbit parameters broadcast by the NNSS satellites. These are as follows: t_p = time of perigee, n = mean motion, ϵ = eccentricity of orbit, ω = argument of perigee at t_p measured in the orbit plane from the XY plane in the positive Z direction, $\dot{\omega}$ = precession rate of ω, A = semimajor axis of orbit, ξ = right ascension of the ascending node measured from the X axis in a counter-clockwise direction in the XY plane (see Fig. 2), $\dot{\xi}$ = precession rate of ξ, i = angle of inclination of satellite orbit, and Λ_G = right ascension of Greenwich at t_p.

By assuming a circular polar orbit we have set $\epsilon = 0$, $i = 90°$, and A = radius of orbit. The time of perigee t_p and the argument of perigee ω become meaningless when applied to a circular orbit; so we will define the satellite period T as the time between two successive ascending nodes.

We can now define the orbit plane by an X_0Y_0 coordinate system, with X_0 in the XY plane making angle ξ with the X axis, and Y_0 coincident with the Z axis. $\mathbf{RS}$ can now be written (Fig. 2)

$$\mathbf{RS} = \mathbf{P}X_0 + \mathbf{Q}Y_0 \tag{5}$$

where the transformation vectors $\mathbf{P}$ and $\mathbf{Q}$ relate the orbit plane X_0Y_0 to the XYZ coordinate system as follows:

$$\begin{aligned} P_x &= \cos\xi,\quad P_y = \sin\xi,\quad P_z = 0 \\ Q_x &= 0,\quad Q_y = 0,\quad Q_z = 1 \end{aligned} \tag{6}$$

The coordinates X_0 and Y_0 can be related to known parameters by

$$X_0 = A\cos E,\quad Y_0 = A\sin E \tag{7}$$